

Research Article

Correlation between the Photocatalytic Degradability of PAHs over Pt/TiO₂-SiO₂ in Water and Their Quantitative Molecular Structure

Zhao-hui Luo,¹ Chuan-ling Wei,¹ Nan-nan He,¹ Zhi-guo Sun,¹ Hui-xin Li,¹ and Dan Chen²

¹College of Resources and Environmental Science, Nanjing Agricultural University, Nanjing 210095, China

²Key Laboratory of Efficient Irrigation-Drainage and Agricultural Soil-Water Environment in Southern China (Ministry of Education), College of Water Conservancy and Hydropower Engineering, Hohai University, Nanjing 210098, China

Correspondence should be addressed to Zhao-hui Luo; lzhui@njau.edu.cn

Received 22 May 2014; Revised 25 July 2014; Accepted 1 August 2014

Academic Editor: Yuekun Lai

Copyright © 2015 Zhao-hui Luo et al. This is an open access article distributed under the Creative Commons Attribution License, which permits unrestricted use, distribution, and reproduction in any medium, provided the original work is properly cited.

The correlation between the photocatalytic degradability of polycyclic aromatic hydrocarbons (PAHs) over Pt/TiO₂-SiO₂ in water and their quantitative molecular structure was studied. Six PAHs, namely, naphthalene, fluorene, phenanthrene, pyrene, benzo[a]pyrene, and dibenzo[a,h]anthracene, were tested in Pt/TiO₂-SiO₂ suspension under UV irradiation. The results showed that the degradation efficiencies of the higher molecular weight PAHs were enhanced significantly in the presence of Pt/TiO₂-SiO₂, while the degradation efficiencies of the lower molecular weight PAHs were decreased in the presence of Pt/TiO₂-SiO₂. Both the photolysis and photocatalysis of all PAHs fit the pseudo-first-order equation very well, except FL. Quantitative analysis of molecular descriptors of energy of the highest occupied molecular orbital (E_{homo}), energy of the lowest unoccupied molecular orbital (E_{lumo}), and the difference between E_{lumo} and E_{homo} , GAP ($\text{GAP} = E_{\text{lumo}} - E_{\text{homo}}$), suggested that the GAP was significant for predicting a PAHs' photocatalytic degradability. Through comparison against the maximum GAP (7.4529 eV) of PAHs (dibenzo[a,h]anthracene) that could be photocatalytically degraded and the minimum GAP (8.2086 eV) of PAHs (pyrene) that could not be photocatalytically degraded in this study, the photocatalytic degradability of 67 PAHs was predicted. The predictions were partly verified by experimental photocatalytic degradation of anthracene and Indeno[1.2.3.cd]pyrene.

1. Introduction

Polycyclic aromatic hydrocarbons (PAHs) are a large group of organic compounds with two or more fused aromatic rings. PAHs are produced mainly by the incomplete combustion of fossil fuels. They are widespread contaminants found in natural bodies of water [1, 2]. Many PAHs have a variety of mutagenic and carcinogenic effects in organisms. It is reported that low molecular weight PAHs (LMW PAHs, compounds containing three or less fused benzene rings) are more susceptible to biodegradation, while high molecular weight PAHs (HMW PAHs, compounds containing four or more fused benzene rings), which are highly mutagenic and carcinogenic, are more recalcitrant [3, 4]. Therefore, it is difficult to eliminate PAHs through traditional biological water treatment [5].

An advanced oxidation technique called TiO₂-photocatalyzed degradation has attracted attention as a method of eliminating a variety of organic compounds because the process can achieve effective mineralization under mild temperature and pressure conditions [6, 7]. Some biorefractory substances, such as norfloxacin [8], dyes [9–11], and 4-chlorocatechol [12], have been reported to degrade successfully using this technique. Some PAHs were also reported to be photocatalytically degraded successfully with the presence of TiO₂ in aqueous environment. Wen et al. [13] examined the photocatalytic degradation of pyrene (PYR) that preadsorbed onto TiO₂ surface before UV irradiation. They found that the pH of the dispersion and the ratio of PYR/TiO₂: water had little effect on the photooxidation rate of PYR, while the extent of surface coverage and the addition of Fe³⁺ affected it greatly. Lin and Valsaraj [14]

studied the degradation of PYR and phenanthrene (PHE) in a dilute water stream by an annular photocatalytic reactor with TiO_2 immobilized on a quartz tube. They found that both PAHs degrade to CO_2 and H_2O in the presence of quinone. Dass et al. [15] found that acenaphthene, anthracene (AN), fluorine (FL), and naphthalene (NP) undergo efficient photocatalytic oxidation in aqueous suspensions of TiO_2 upon irradiation with a 500 W super-high pressure mercury lamp as well as sunlight. Lair et al. [16] studied the degradation of NP in water by photocatalysis in UV-irradiated TiO_2 suspensions. They found that the optimum TiO_2 was 2.5 g L^{-1} . They also observed that CO_3^{2-} strongly inhibited NP adsorption and removal, while pH had insignificant effect upon the NP removal, and temperature slightly accelerated the NP degradation. Through the identification of the main intermediates of NP photodegradation, they proposed that NP degraded by oxygenated radicals and by direct oxidation in the holes formed. Woo et al. [17] investigated the effects of acetone on the photocatalytic degradation efficiency and pathways of NP, acenaphthylene (ACN), PHE, AN, and benzo[a]anthracene in synthetic water. They observed that PAHs photolysis generated toxic intermediate products, especially in the case of ACN and PHE. However, all PAHs complete detoxification was achieved in a 24 h of UV/ TiO_2 system by 100 mg L^{-1} of catalyst. They also found that acetone enhanced PAHs degradation, but 16% acetone addition significantly altered the degradation pathway of NP and ACN. Vela et al. [18] investigated the removal of a mixture of six PAHs (BaP, benzo[b]fluoranthene, benzo[ghi]perylene, benzo[k]fluoranthene, fluoranthene, and InP) from groundwater by ZnO and TiO_2 photocatalysis in tandem with $\text{Na}_2\text{S}_2\text{O}_8$ as oxidant under natural sunlight. The photocatalytic experiments showed that the addition of photocatalyst strongly improved the elimination of PAHs in comparison with photolytic tests. The time required for 90% degradation in the condition of the study was in the ranges 7–15 min and 18–76 min for ZnO and TiO_2 systems, respectively.

Although the TiO_2 -photocatalyzed degradation technology has been extensively investigated in pollutant treatment in the last two decades, its practical application is limited because of the disadvantages of TiO_2 , such as its low surface area, low adsorbability for pollutants, fast recombination of photogenerated electrons-hole pair, the maximum absorption in the ultraviolet light region, and the difficulty of separation from treated water [19, 20]. Numerous approaches, such as composite semiconductor, noble metal loading, ion doping, nanotube formation, and sensitization, have been used to modify TiO_2 to overcome the above disadvantages [21–24]. SiO_2 is one of the most popular coupled materials in composite semiconductors. Mixed TiO_2 - SiO_2 has been reported to be three times more photoactive than TiO_2 alone [25]. The addition of SiO_2 particles not only alters the size and shape of the TiO_2 particles, but also increases the thermal stability and adsorbability of TiO_2 particles [26, 27]. Platinum (Pt) is one of the most common noble metals loading on TiO_2 . Ishibai et al. [28] reported their Pt- TiO_2 possessed high photocatalytic activity under visible light irradiation, as well as under UV light irradiation.

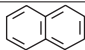
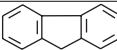
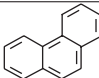
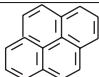
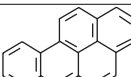
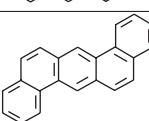
They suggested that the surface complex formation associated with Ti-O-Pt chemisorption dominated the visible light reactivity. Devipriya et al. [29] prepared Pt- TiO_2 and immobilized it on ceramic tiles. They found that the catalyst was effective for the solar photocatalytic removal of chemical and bacterial pollutants from water. The optimum loading of Pt on TiO_2 was found to be 0.5%. Ahmed et al. [30] reported that their Pt- TiO_2 samples are more active than the corresponding bare TiO_2 for both methanol oxidation and dehydrogenation processes. The particle size of Pt- TiO_2 was decreased with the increasing of platinum loading. Some researchers attributed the enhanced photocatalytic activity to the increased light absorption and the retardation of the photogenerated electron-hole recombination [30, 31]. As the Fermi level of Pt is lower than that of TiO_2 , photoexcited electrons can be transferred from conduction band to Pt particles deposited on the surface of TiO_2 , while photogenerated valence band holes remain on the TiO_2 . These activities greatly reduce the possibility of electron-hole recombination, resulting in stronger photocatalytic reactions [31].

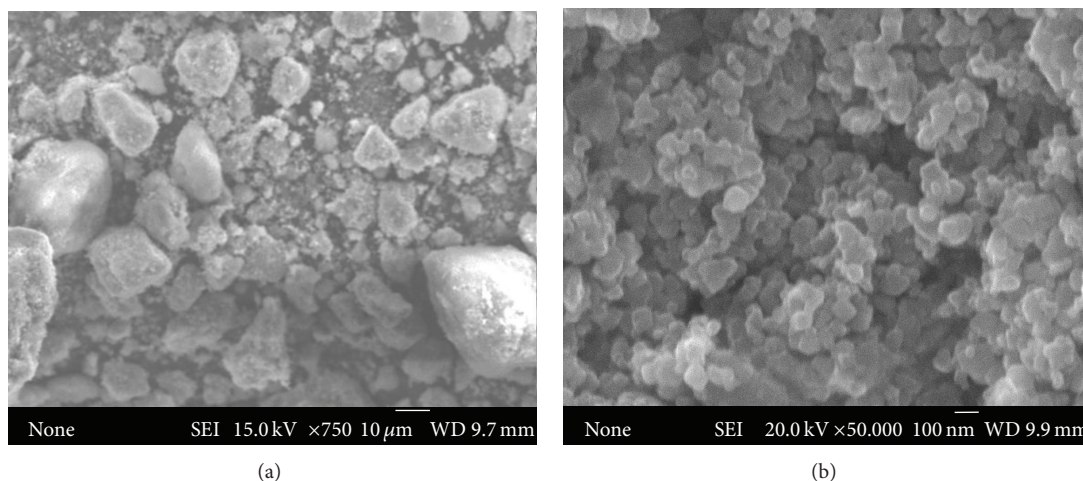
Our previous works proved that a porous photocatalyst Pt/ TiO_2 - SiO_2 could efficiently decompose PYR, a four-ring PAH [34, 35]. It was also interesting to know the efficiency of Pt/ TiO_2 - SiO_2 for decomposing other PAHs. However, the PAH group of organic compounds is very large (over 100 toxic compounds). It would consume much time and money to identify the degradability of all PAHs in Pt/ TiO_2 - SiO_2 suspension. To solve this problem, quantitative structure activity relationships (QSAR) modeling, which correlates and predicts transport and transformation process data of organic pollution from their structural descriptors, may be used to study photocatalysis mechanisms and generate predicted photocatalysis process data efficiently [36, 37].

It is greatly important to develop QSAR models in which quantum chemical descriptors are used. Quantum chemical descriptors clearly describe defined molecular properties. They can easily be obtained by computation. Lu et al. [38] studied QSAR of phenols and anilines for predicting the toxicity of these compounds to algae. Hu and Aizawa [39] studied the QSAR for the estrogen receptor binding affinity of phenolic chemicals. de Lima Ribeiro and Ferreira [40] studied the QSAR of 67 PAHs in order to predict the phototoxicity of these compounds. Chen et al. [41–44] studied the QSAR in order to predict the photolysis of PAHs and dibenzo-p-dioxin. In the above studies, the quantum chemical descriptors of energy of the highest occupied molecular orbital (E_{homo}), the energy of the lowest unoccupied molecular orbital (E_{lumo}), and the GAP, the difference between E_{lumo} and E_{homo} ($\text{GAP} = E_{\text{lumo}} - E_{\text{homo}}$), were proven to be significant for PAH photochemical QSAR studies [43, 45, 46]. E_{lumo} and E_{homo} can serve as measures of the molecular capacity to donate or to accept an electron pair, respectively. The GAP expresses the necessary energy to excite an electron from HOMO to LUMO [40]. These descriptors can be obtained by semiempirical molecular orbital algorithms [40, 47].

The present study aimed to further understand the function of Pt/ TiO_2 - SiO_2 and to investigate the photocatalytic degradation character and kinetics of PAHs. Six PAHs were tested in Pt/ TiO_2 - SiO_2 suspension. The PAHs included three

TABLE 1: Physicochemical properties of NP, FL, PHE, PYR, BaP, and DahA [32, 33].

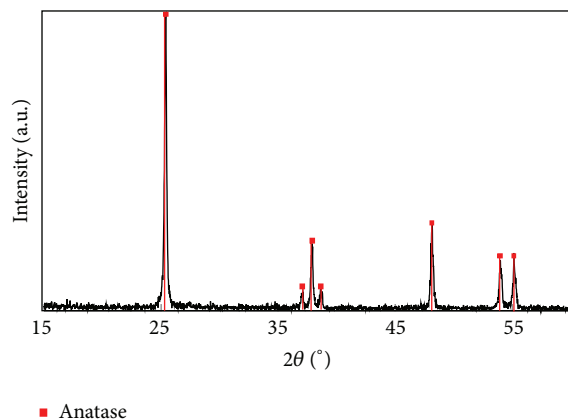
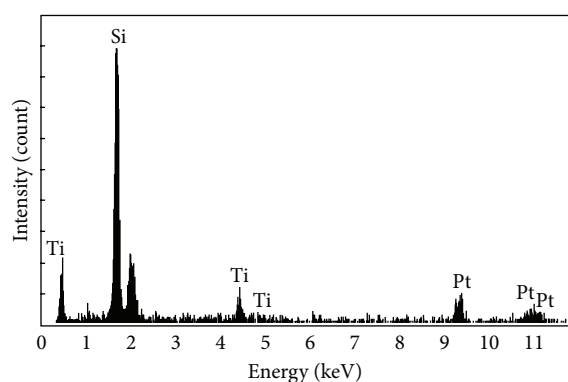
PAHs	Chemical structures	Mr	Molecular formula	CAS number	Solubility (mmol L ⁻¹)	log K_{ow}	Vapor pressure 25°C (Pa)	K_H (amt m ³ mol ⁻¹)
NP		128	C ₁₀ H ₈	91-20-3	2.4×10^{-1}	3.37	10.9	4.5×10^{-3}
FL		166	C ₁₃ H ₁₀	86-73-7	1.2×10^{-2}	4.18	8.81×10^{-2}	7.4×10^{-5}
PHE		178	C ₁₄ H ₁₀	85-01-8	7.2×10^{-3}	4.45	1.6×10^{-2}	2.7×10^{-4}
PYR		202	C ₁₆ H ₁₀	129-00-0	7.2×10^{-4}	4.88	8.86×10^{-4}	1.3×10^{-5}
BaP		252	C ₂₀ H ₁₂	50-32-8	8.4×10^{-7}	6.06	1.5×10^{-5}	7.4×10^{-5}
DahA		278	C ₂₂ H ₁₂	53-70-3	$(3.7 \pm 1.8) \times 10^{-10}$	6.50	0.8×10^{-6}	2.0×10^{-9}

FIGURE 1: SEM images of Pt/TiO₂-SiO₂; magnification power is (a) 750 and (b) 50,000.

LMW PAHs, NP, FL, and PHE, and three HMW PAHs, PYR, benzo[a]pyrene (BaP), and dibenzo[a,h]anthracene (DahA). The selected PAHs are frequently detected in natural bodies of water [1, 2, 48]. The HMW PAHs are all acutely carcinogenic PAHs. The physicochemical properties of the selected PAHs are listed in Table 1. The degradation kinetics for photocatalytically degradable PAHs were also studied. E_{lumo} , E_{homo} , and GAP were adopted as the molecular descriptors for NP, FL, PHE, PYR, BaP, and DahA. They have been calculated in a previous research [40]. Based upon the results, the primary correlation between the photocatalytic degradability of PAHs over Pt/TiO₂-SiO₂ in water and their quantitative molecular structure was studied. Based upon the analysis of correlation, the photocatalytic degradability of 67 PAHs was predicted, and the predictions were partly verified by experiments of photocatalytic degradation of anthracene (AN) and Indeno[1.2.3.cd]pyrene (InP).

2. Experimental Section

2.1. Materials and Reagents. All reagents were of analytical quality, and all solvents were of HPLC grade. All PAHs were purchased from Kanto Chemical Co., Inc., (Japan). The Pt/TiO₂-SiO₂ used in the present study was synthesized by the method presented in previous work [35] under a compaction pressure of 1.83×10^5 kPa, Pt coating ratio of 0.4 wt%, TiO₂:SiO₂ of 1:1, and calcination temperature of 973 K. The scanning electron microscopy (SEM) images (Figure 1) show the surface roughness and morphology of Pt/TiO₂-SiO₂. The X-ray diffraction (XRD) and the energy-dispersive analysis of the X-ray (EDAX) analysis could give some interesting information of the structure of Pt/TiO₂-SiO₂. The XRD spectrum (Figure 2) indicates that TiO₂ in Pt/TiO₂-SiO₂ is in anatase form, and EDAX spectrum (Figure 3) shows the compositions of Pt/TiO₂-SiO₂.

FIGURE 2: XRD spectrum of Pt/TiO₂-SiO₂.FIGURE 3: EDAX spectrum of Pt/TiO₂-SiO₂.

2.2. Photocatalytic Degradation of PAHs. The reaction solutions were prepared by introducing a proper volume of stock solution (50 mg L⁻¹) into a water/methanol (99/1) solvent to achieve a required final concentration. Water was purified by Milli-Q Plus system (Millipore). Methanol (1%) was added to minimize the adsorption of PAHs to the glassware walls. The reaction mixture was 100 mL of initial concentration of PAHs at 5×10^{-8} M and 0.3 g L⁻¹ of Pt/TiO₂-SiO₂ in a glass beaker, continuously mixed with a magnetic stirrer. A black-light lamp (27 w) emitting monochromatic radiation at 368 nm was placed above the reaction solution. The distance between the lamp and the surface of the solution was 5 cm. Before irradiation, the solution was stirred in the dark for 30 min to allow the system to reach adsorption equilibrium.

A sample approximately 2 mL was taken at the designed time interval during irradiation. The same volume of ethanol was added to the sample to prevent the loss of PAHs on wall of glassware, and then it was centrifuged and filtered through a 0.45 μm cellulose filter to remove all solid particles. The treated sample was analyzed by high-performance liquid chromatography (HPLC; Hitachi L-7300 HPLC) with a fluorescence detector Hitachi L-7485. The chromatography equipment was equipped with a C-18-reversed phase separation column and the mobile phase was a 90/10 volumetric ratio mixture of methanol/water. The detecting wavelengths for NA, FL, PHE, PYR, BaP, DahA, AN, and InP were 216/308,

210/310, 248/365, 245/390, 297/430, 286/430, 297/390, and 300/500 nm (excitation/emission nm), respectively.

2.3. Photocatalytic Degradation Kinetics of PAHs. Pseudo-first-order kinetics (1) is normally assumed for PAH photolysis [12, 49]:

$$-\frac{d(C)}{dt} = kC. \quad (1)$$

Therefore, the rate constant and half-life time of PAHs degradation were calculated using the following equations:

$$\ln \frac{C_0}{C} = kt, \quad (2)$$

$$t_{1/2} = \frac{\ln 2}{K},$$

where C_0 and C are PAHs' concentration at times zero and t , respectively, k is the rate constant, and $t_{1/2}$ is the half-life time.

2.4. Data Set of Quantitative Molecular Structure of PAHs. The present work studied 67 nonsubstituted PAHs containing 2–7 rings with 5 and 6 carbon atoms (Figure 4). The electronic descriptors of E_{lumo} , E_{homo} , and the GAP for PAHs obtained using the AM1 algorithm reported by de Lima Ribeiro and Ferreira [40] were selected in this study.

3. Results and Discussion

3.1. Photocatalytic Degradation of PAHs in Pt/TiO₂-SiO₂ Suspension. The photolysis and photocatalysis of the selected PAHs are shown in Figure 5. It was observed that Pt/TiO₂-SiO₂ played a very different role in photocatalysis of LMW PAHs and HMW PAHs. The presence of Pt/TiO₂-SiO₂ increased the degradation rates of HMW PAHs efficiently, while the presence of Pt/TiO₂-SiO₂ inhibited the degradation rates of LMW PAHs. Similar results were obtained in previous research, which confirms that the presence of TiO₂ resulted in a slower photooxidation rate of FL [50]. This difference is considered to be related to the PAHs' molecular structure, which determines the reactivity of a PAH.

3.2. Kinetics of Photocatalytic Degradation of PAHs. The pseudo-first-order kinetics equation, rate constant, half-life time, correlation coefficients, and total removal efficiency of photolysis and photocatalysis of selected PAHs are summarized in Table 2. The results show that the total removal efficiencies of photocatalysis for NP, FL, and PHE are 4.8%, 24.7%, and 34.5%, respectively, lower than the photolysis removal efficiencies of 46.6%, 41.5%, and 41.9%, respectively. On the other hand, the total removal efficiencies of photocatalysis for PYR, BaP, and DahA were 81.4%, 99.7%, and 88.6%, respectively, all higher than the photolysis removal efficiency of 37.8%, 99.0%, and 71.8%, respectively. The rate constant of the tested PAHs presents the same phenomenon. The rate constant of photocatalysis of NP, FL, and PHE is 0.0006, 0.0021, and 0.0038, respectively, lower than the photolysis removal efficiency of 0.0054, 0.0035, and 0.0046.

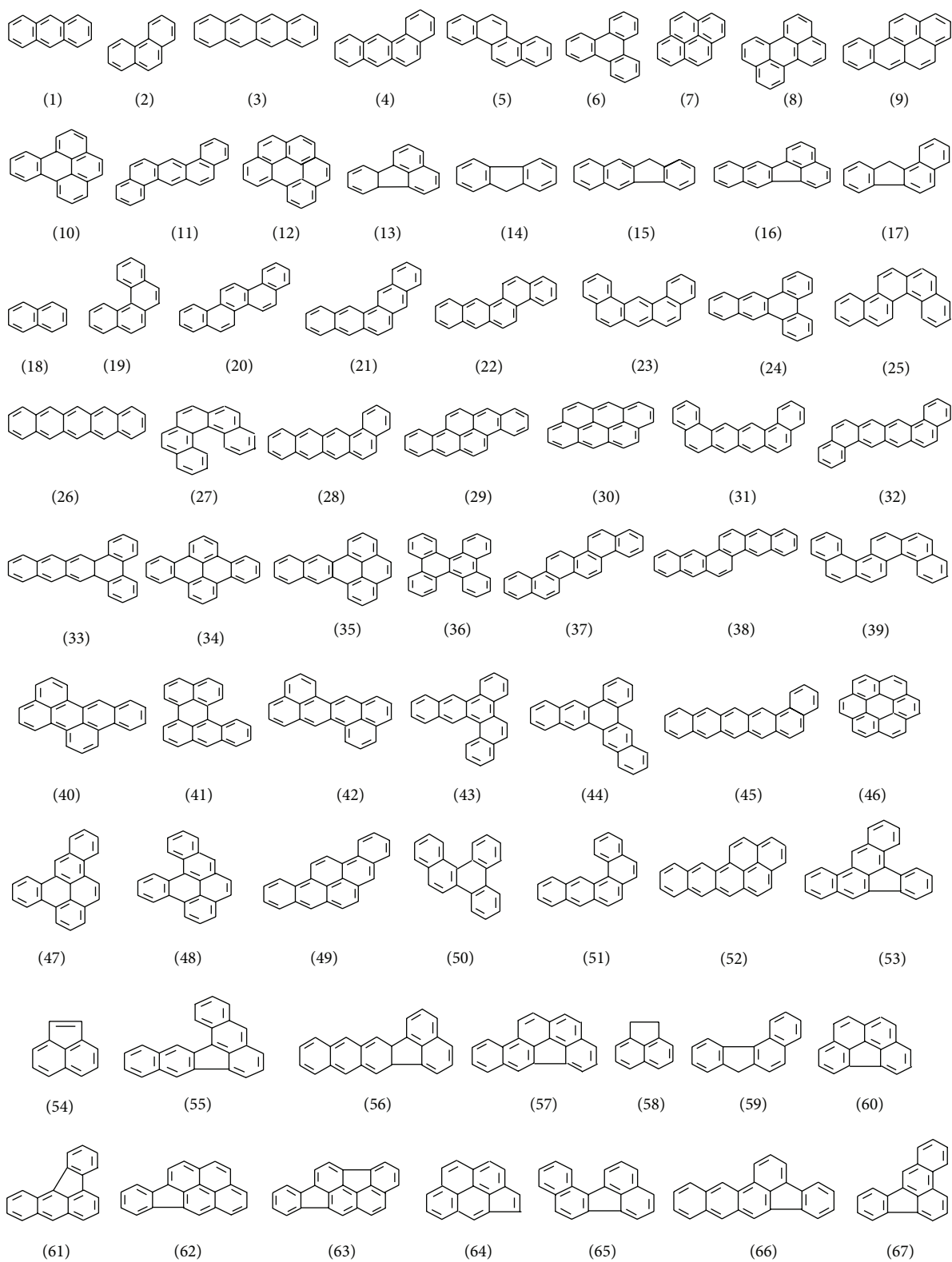


FIGURE 4: Chemical structures of PAHs [40].

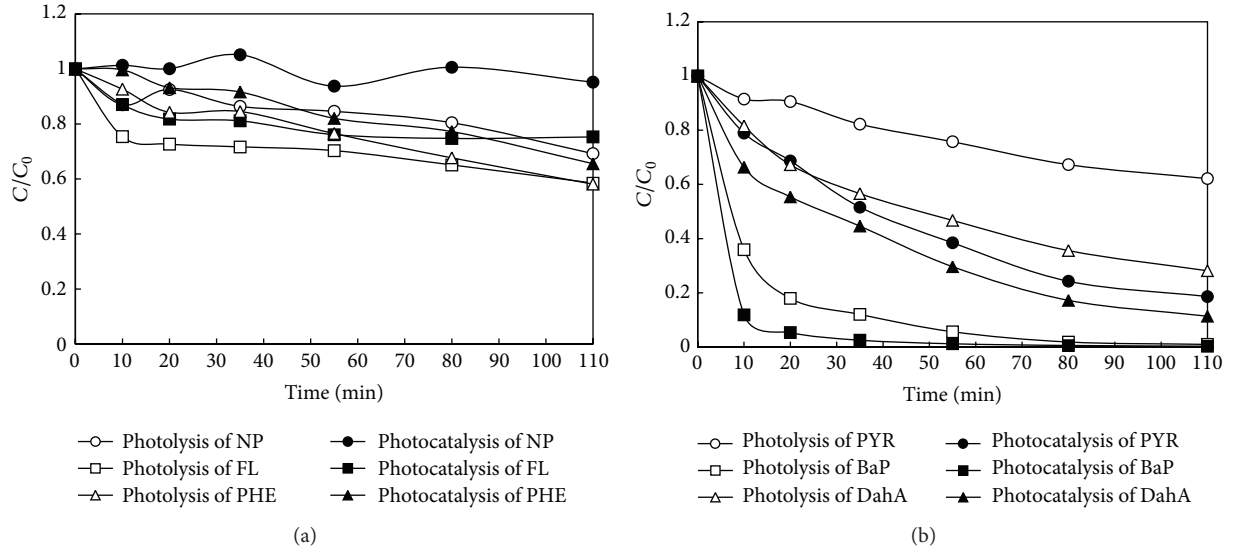


FIGURE 5: The photolysis and photocatalysis of (a) LMW PAHs: NP, FL, and PHE and (b) HMW PAHs: PYR, BaP, and DahA.

TABLE 2: Pseudo-first-order regression equation, correlation coefficient, rate constant, half-life time, and the total removal efficiency of photolysis and photocatalysis of PYR, BaP, and DahA (initial concentration: 5×10^{-8} M).

Treatment	PAHs	Regression equation	$t_{1/2}$ (min)	K (min^{-1})	R^2	Removal efficiency (%)
Photolysis	NP	$y = 0.0054x + 0.0259$	128.4	0.0054	0.9905	46.6
	FL	$y = 0.0035x + 0.1646$	198.0	0.0035	0.7332	41.5
	PHE	$y = 0.0046x + 0.0258$	150.7	0.0046	0.9802	41.9
	PYR	$y = 0.0043x + 0.0278$	161.2	0.0043	0.9833	37.8
	BaP	$y = 0.0398x + 0.5683$	17.4	0.0398	0.958	99.0
	DahA	$y = 0.0112x + 0.1094$	61.9	0.0112	0.9767	71.8
Photocatalysis	NP	$y = 0.0006x - 0.0111$	1155.2	0.0006	0.9093	4.8
	FL	$y = 0.0021x + 0.1047$	330.1	0.0021	0.6774	24.7
	PHE	$y = 0.0038x - 0.0211$	182.4	0.0038	0.9803	34.5
	PYR	$y = 0.0155x + 0.0731$	44.7	0.0155	0.9878	81.4
	BaP	$y = 0.0452x + 1.433$	15.3	0.0452	0.8443	99.7
	DahA	$y = 0.0192x + 0.1435$	36.1	0.0192	0.9878	88.6

On the contrary, the rate constant of photocatalysis for PYR, BaP, and DahA of 0.0155, 0.0452, and 0.0192, respectively, is all higher than the rate constant of 0.0043, 0.0398, and 0.0112, respectively.

The correlation coefficients indicate that both the photolysis and photocatalysis of PAHs fit the pseudo-first-order equation very well, except FL, for which the R^2 for photolysis and photocatalysis are 0.7332 and 0.6774, respectively. This might be attributed to the special molecular structure of FL, which is the only PAH with a 5-carbon ring structure and which has the largest GAP value of 8.5021 eV among the tested PAHs (see Section 3.3), resulting in a more difficult photoinduced reaction for FL. The results indicate that the photolytic and photocatalytic degradation mechanisms of FL are different from that of other tested PAHs.

3.3. E_{lumo} , E_{homo} , and GAP of PAHs. The E_{lumo} , E_{homo} , and GAP of NP, FL, PHE, PYR, BaP, and DahA obtained by AM1

algorithm in de Lima Ribeiro and Ferreira research [40] are summarized in Table 3.

It is observed that the values of E_{homo} of HMW PAHs are all higher than those of LMW PAHs. On the contrary, the GAP values of HMW PAHs molecular are all lower than those of LMW PAHs. The GAP values of the PAHs for which degradation could be accelerated by Pt/TiO₂-SiO₂ are all smaller than or equal to 7.4529 eV; on the other hand, the GAP values of PAHs for which degradation was inhibited by Pt/TiO₂-SiO₂ are all larger than or equal to 8.2086 eV. These results indicate that more photoenergy is required for triggering the degradation of LMW PAHs than that of HMW PAHs. It can be understood that GAP values can serve as a measure of the excitability of the molecule: the smaller the GAP of a PAH, the easier it will be excited.

3.4. Prediction of the Photocatalytic Degradability of 67 PAHs. The photochemical properties of PAHs undoubtedly depend

TABLE 3: Summary of E_{lumo} , E_{homo} , and GAP for NP, FL, PHE, PYR, BaP, and DahA.

	NP	FL	PHE	PYR	BaP	DahA
HOMO (eV)	-8.7099	-8.7109	-8.6171	-8.0692	-7.9173	-8.2570
LUMO (eV)	-0.2650	-0.2088	-0.4085	-0.9225	-1.1142	-0.8041
GAP (eV)	8.4449	8.5021	8.2086	7.1467	6.8031	7.4529
Degradation accelerated by Pt/TiO ₂ -SiO ₂	No	No	No	Yes	Yes	Yes

upon their molecule excitability; therefore, the GAP value is expected to predict the photocatalytic degradability of other PAHs in Pt/TiO₂-SiO₂ suspension.

As mentioned above, the maximum GAP of DahA of tested PAHs for which degradation could be accelerated by Pt/TiO₂-SiO₂ was 7.4529 eV, and the minimum GAP of PHE of tested PAHs for which degradation was accelerated by Pt/TiO₂-SiO₂ was 8.2086 eV. Therefore, one can deduce that when the GAP of a PAH is less than or equal to 7.4529 eV, this PAH can be degraded in Pt/TiO₂-SiO₂-UV system. On the other hand, when the GAP of a PAH is larger than or equal to 8.2086 eV, this PAH cannot be degraded in Pt/TiO₂-SiO₂-UV system. When the GAP of a PAH is between 7.4529 eV and 8.2086 eV, the degradation potential of this PAH is uncertain in the experimental condition of our study.

Following the above approach, the photocatalytic degradability of 67 PAHs was predicted and is listed in Table 4. The results show that 46 PAHs are potentially photocatalytically degradable. All of these 46 PAHs, except AN (anthracene, labelled no. 1), were all HMW PAHs. There were four PAHs for which no photocatalytic degradability was predicted. All four of these PAHs were LMW PAHs (labelled nos. 2, 14, 18, and 58). For these LMW PAHs, biological treatment can be a very good complement [51, 52]. The photocatalytic degradability of another seventeen PAHs was determined to be uncertain, most of which were 4~6-ring PAHs.

3.5. Verification of Prediction. To verify the above prediction, the photolysis and photocatalysis of AN (number 1, 3-ring PAH) and InP (number 62, 6-ring PAH), whose GAPs are 7.2795 eV and 6.8528 eV, respectively, were examined in Pt/TiO₂-SiO₂-UV system. We selected AN and InP because they are also PAHs commonly found in water [18, 53], and AN is the only LMW PAH which is assumed to be photocatalytically degradable. If the prediction was right, the degradation of these two PAHs should be accelerated in the Pt/TiO₂-SiO₂-UV system. It is shown clearly in Figure 6 that the degradation rate of AN and InP is indeed improved with the presence of Pt/TiO₂-SiO₂. The photocatalytic degradation of AN and InP in the Pt/TiO₂-SiO₂-UV system can also be described by the first-order kinetic model. The rate constant, half-life time, and the total removal efficiency of photocatalysis for AN are 0.0766 min⁻¹, 9.05 min, and 100%, respectively, while those for InP were 0.0079 min⁻¹, 87.74 min, and 63.11%, respectively. Therefore, the prediction is verified in a way.

For further study, the determination of photocatalytic degradability for the remaining PAHs can be identified by setting a new boundary value of GAP, which can be obtained by appropriate testing of the uncertain PAHs.

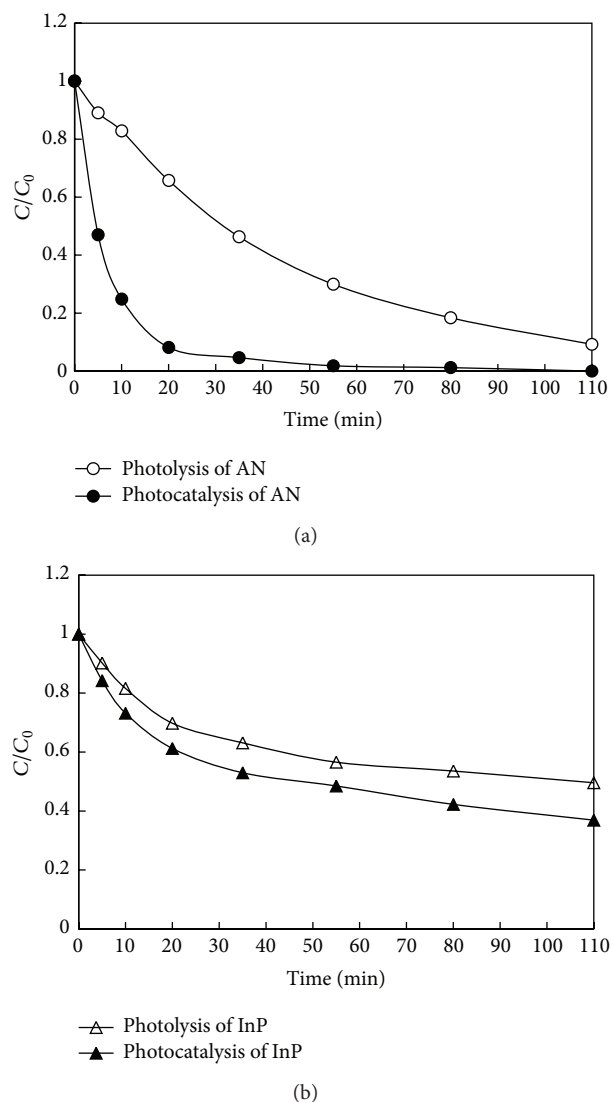


FIGURE 6: The photolysis and photocatalysis of (a) AN and (b) InP. Initial concentration is 5×10^{-8} M.

The prediction is significant for realistic water treatment. By knowing the value of GAP, the photocatalytic degradability of some pollutants in the photocatalyst suspension might be known without doing any experimentation. The GAP value can be obtained easily from previous research or by computation. Therefore, large expenditures of time and money required for the determination can be avoided.

TABLE 4: Evaluation of photocatalytic degradability of 67 PAHs.

	PAHs name	E_{lumo} (eV)	E_{homo} (eV)	GAP (eV)	Photocatalytic degradability	
1	<i>Anthracene</i>	−0.8417	−8.1212	7.2795	○	
2	Phenanthrene	−0.4085	−8.6171	8.2086		×
3	Naphthacene	−1.2321	−7.7488	6.5167	○	
4	Benz[a]anthracene	−0.8116	−8.2079	7.3963	○	
5	Chrysene	−0.6762	−8.3697	7.6935		△
6	Triphenylene	−0.4532	−8.6584	8.2052		△
7	Pyrene	−0.9225	−8.0692	7.1467	○	
8	Perylene	−1.1508	−7.8598	6.7090	○	
9	Benzo[a]pyrene	−1.1142	−7.9173	6.8031	○	
10	Benzo[e]pyrene	−0.8580	−8.2149	7.3569	○	
11	Dibenz[a,h]anthracene	−0.8041	−8.257	7.4529	○	
12	Benzo[ghi]perylene	−1.0662	−8.0235	6.9573	○	
13	Fluoranthene	−0.9294	−8.6301	7.7007		△
14	Fluorene	−0.2088	−8.7109	8.5021		×
15	Benzo[b]fluorene	−0.4880	−8.4783	7.9903		△
16	Benzo[k]fluoranthene	−1.1769	−8.3164	7.1395	○	
17	Benzo[a]fluorene	−0.5607	−8.3656	7.8049		△
18	Naphthalene	−0.2650	−8.7099	8.4449		×
19	Benzo[c]phenanthrene	−0.6456	−8.4438	7.7982		△
20	Picene	−0.7209	−8.3487	7.6278		△
21	Pentaphene	−0.8400	−8.2022	7.3622	○	
22	Benzo[b]chrysene	−0.9948	−8.0511	7.0563	○	
23	Dibenz[a, j]anthracene	−0.8736	−8.1916	7.3180	○	
24	Benzo[b]triphenylene	−0.8319	−8.2255	7.3936	○	
25	Benzo[c]chrysene	−0.6931	−8.3898	7.6967		△
26	Pentacene	−1.5500	−7.4414	5.8914	○	
27	Dibenzo[c, g]phenanthrene	−0.6732	−8.3498	7.6766		△
28	Benzo[a]naphthacene	−1.1857	−7.8407	6.6550	○	
29	Dibenzo[b, def]chrysene	−1.3630	−7.6784	6.3154	○	
30	Dibenzo[def, mno]chrysene	−1.4067	−7.6315	6.2248	○	
31	Dibenzo[a, j]naphthacene	−1.1349	−7.9321	6.7972	○	
32	Dibenzo[a, l]naphthacene	−1.1352	−7.9345	6.7993	○	
33	Dibenzo[a, c]naphthacene	−1.1564	−7.9148	6.7584	○	
34	Dibenzo[el]naphthacene	−0.8276	−8.2948	7.4672		△
35	Dibenzo[de, gr]naphthacene	−0.8336	−8.2774	7.4438	○	
36	Dibenzo[g, p]chrysene	−0.8832	−8.1128	7.2296	○	
37	Benzo[c]picene	−0.8279	−8.2597	7.4318	○	
38	Dibenzo[b, k]chrysene	−1.1775	−7.8832	6.7057	○	
39	Dibenzo[cl]chrysene	−0.7827	−8.2649	7.4822		△
40	Benzo[b]perylene	−1.1806	−7.8666	6.686	○	
41	Benzo[a]perylene	−1.4836	−7.5284	6.0448	○	
42	Dibenzo[de, mn]naphthacene	−1.5482	−7.4305	5.8823	○	
43	Naphtho[2,3-g]chrysene	−0.9944	−8.1177	7.1233	○	
44	Benzo[h]pentaphene	−0.8089	−8.3009	7.4920		△
45	Benzo[a]pentacene	−1.4685	−7.5763	6.1078	○	
46	Coronene	−1.0021	−8.1438	7.1417	○	
47	Naphtho[1,2,3,4-def]chrysene	−1.0583	−8.0233	6.9650	○	
48	Dibenzo[def, p]chrysene	−1.1022	−7.9553	6.8531	○	
49	Benzo[rst]pentaphene	−1.1838	−7.865	6.6812	○	
50	Benzo[g]chrysene	−0.7660	−8.2705	7.5045		△

TABLE 4: Continued.

	PAHs name	E_{lumo} (eV)	E_{homo} (eV)	GAP (eV)	Photocatalytic degradability		
51	2,3:5,6-Dibenzophenanthrene	−0.9636	−8.0436	7.0800	○		
52	Naphtho[2.1.8- <i>qra</i>]-naphthacene	−1.3169	−7.7299	6.4130	○		
53	Dibenz[<i>a.e</i>]aceanthrylene	−1.2806	−8.1423	6.8617	○		
54	Acenaphthylene	−0.9359	−8.9429	8.0070		△	
55	Dibenzo[<i>a.k</i>]fluoranthene	−1.2992	−7.9435	6.6443	○		
56	Naphtho[2.3- <i>k</i>]fluoranthene	−0.9127	−7.9781	7.0654	○		
57	Dibenzo[<i>k.mno</i>]fluoranthene	−0.9755	−8.4001	7.4246	○		
58	1,2-Dihydroacenaphthylene	−0.2132	−8.4945	8.2813			×
59	Benzo[<i>c</i>]fluorene	−0.6415	−8.2836	7.6421		△	
60	Benzo[<i>ghi</i>]fluoranthene	−0.9911	−8.6996	7.7085		△	
61	Benzo[<i>a</i>]aceanthrylene	−1.3219	−8.085	6.7631	○		
62	Indeno[1.2.3- <i>cd</i>]pyrene	−1.2835	−8.1363	6.8528	○		
63	Indeno[1.2.3- <i>cd</i>]fluoranthene	−1.3350	−8.5435	7.2085	○		
64	Cyclopenta[<i>cd</i>]pyrene	−1.3123	−8.2727	6.9604	○		
65	Benzo[<i>j</i>]fluoranthene	−1.1767	−8.3165	7.1398	○		
66	Dibenz[<i>e.k</i>]acephenanthrylene	−1.0702	−8.2215	7.1513	○		
67	Benzo[<i>b</i>]fluoranthene	−0.9654	−8.6166	7.6512		△	
Total		—	—	—	46	17	4

(○) means having photocatalytic degradability ($\text{GAP} \leq 7.4529$ eV); (△) means having indeterminate photocatalytic degradability (7.4529 eV $\leq \text{GAP} \leq 8.2086$ eV); (×) means having nonphotocatalytic degradability.

4. Conclusions

The present study was undertaken to probe the correlation between the photocatalytic degradability of PAHs over Pt/TiO₂-SiO₂ in water and their quantitative molecular structure. Six PAHs, NP, FL, PHE, PYR, BaP, and DahA, were experimentally tested in a Pt/TiO₂-SiO₂ suspension under UV irradiation. The results show that the degradation of HMW PAHs, PYR, BaP, and DahA, was accelerated significantly in the presence of Pt/TiO₂-SiO₂, while the degradation efficiency of low molecular weight PAHs, NP, FL and PHE, was inhibited under the same experimental conditions. Both the photolysis and photocatalysis of PAHs fit the pseudo-first-order equation very well, except FL. This might be attributed to FL's 5-carbon ring structure. Quantitative analysis of molecular descriptors of E_{lumo} , E_{homo} , and GAP suggested that GAP was significant for predicting PAHs' photocatalytic degradability. By comparing to the maximum GAP (7.4529 eV) of PAHs (DahA) that could be photocatalytically degraded and the minimum GAP (8.2086 eV) of PAHs (PHE) that could not be photocatalytically degraded in this study, the photocatalytic degradability of 67 PAHs was predicted: 46 PAHs were potentially photocatalytically degradable, 4 PAHs were predicted to be not photocatalytically degradable, and 17 PAHs were predicted to exhibit indeterminate photocatalytic degradation. The experiments of photocatalytic degradation of AN and InP verified the above prediction. This prediction indicates that Pt/TiO₂-SiO₂ can offer a very promising method for biorefractory HMW PAHs removal. It can also be a very good complement for biological treatment of PAH contaminated water.

Conflict of Interests

The authors of the paper do not have a direct financial relation with the commercial identity mentioned in this paper that might lead to a conflict of interests.

Acknowledgments

The authors extend sincere thanks to the National Natural Science Foundation of China (Grant no. 51109108), the Natural Science Foundation of Jiangsu province (Grant no. BK2011654), the Science Foundation for Young Scholars of Nanjing Agricultural University (Grant no. KJ2010005), the Natural Science Foundation of Jiangsu Province (PAPD), and the Technology Foundation for Selected Overseas Chinese Scholar, for their support, and the project sponsored by the Scientific Research Foundation for the Returned Overseas Chinese Scholars, State Education Ministry.

References

- [1] G. Guo, F. Wu, H. He, R. Zhang, H. Li, and C. Feng, "Distribution characteristics and ecological risk assessment of PAHs in surface waters of China," *Science China Earth Sciences*, vol. 55, no. 6, pp. 914–925, 2012.
- [2] N. U. Benson, J. P. Essien, F. E. Asuquo, and A. L. Eritobor, "Occurrence and distribution of polycyclic aromatic hydrocarbons in surface microlayer and subsurface seawater of Lagos Lagoon, Nigeria," *Environmental Monitoring and Assessment*, vol. 186, no. 9, pp. 5519–5529, 2014.

- [3] L. N. Ukiwe, U. U. Egereonu, P. C. Njoku, C. I. A. Nwoko, and J. I. Allinor, "Polycyclic aromatic hydrocarbons degradation techniques: a review," *International Journal of Chemistry*, vol. 5, no. 4, pp. 43–55, 2013.
- [4] K. M. Koran, M. T. Suidan, A. P. Khodadoust, G. A. Sorial, and R. C. Brenner, "Effectiveness of an anaerobic granular activated carbon fluidized-bed bioreactor to treat soil wash fluids: a proposed strategy for remediating PCP/PAH contaminated soils," *Water Research*, vol. 35, no. 10, pp. 2363–2370, 2001.
- [5] A. Rubio-Clemente, R. A. Torres-Palma, and G. A. Peñuela, "Removal of polycyclic aromatic hydrocarbons in aqueous environment by chemical treatments: a review," *Science of the Total Environment*, vol. 478, pp. 201–225, 2014.
- [6] A. di Paola, E. García-López, G. Marci, and L. Palmisano, "A survey of photocatalytic materials for environmental remediation," *Journal of Hazardous Materials*, vol. 211–212, pp. 3–29, 2012.
- [7] I. Fechete, Y. Wang, and J. C. Védrine, "The past, present and future of heterogeneous catalysis," *Catalysis Today*, vol. 189, no. 1, pp. 2–27, 2012.
- [8] M. R. Haque and M. Muneer, "Photodegradation of norfloxacin in aqueous suspensions of titanium dioxide," *Journal of Hazardous Materials*, vol. 145, no. 1–2, pp. 51–57, 2007.
- [9] T. Jagadale, M. Kulkarni, D. Pravarthana, W. Ramadan, and P. Thakur, "Photocatalytic degradation of azo dyes using Au:TiO₂, γ -Fe₂O₃:TiO₂ functional nanosystems," *Journal of Nanoscience and Nanotechnology*, vol. 12, no. 2, pp. 928–936, 2012.
- [10] N. Muhd Julkapli, S. Bagheri, and S. Abd Hamid, "Recent advances in heterogeneous photocatalytic decolorization of synthetic dyes," *The Scientific World Journal*, vol. 2014, Article ID 692307, 25 pages, 2014.
- [11] S. Kurinobu, K. Tsurusaki, Y. Natui, M. Kimata, and M. Hasegawa, "Decomposition of pollutants in wastewater using magnetic photocatalyst particles," *Journal of Magnetism and Magnetic Materials*, vol. 310, no. 2, part 3, pp. e1025–e1027, 2007.
- [12] A. Dhir, N. T. Prakash, and D. Sud, "Comparative studies on TiO₂/ZnO photocatalyzed degradation of 4-chlorocatechol and bleach mill effluents," *Desalination and Water Treatment*, vol. 46, no. 1–3, pp. 196–204, 2012.
- [13] S. Wen, J. Zhao, G. Sheng, J. Fu, and P. Peng, "Photocatalytic reactions of pyrene at TiO₂/water interfaces," *Chemosphere*, vol. 50, no. 1, pp. 111–119, 2003.
- [14] H. F. Lin and K. T. Valsaraj, "A titania thin film annular photocatalytic reactor for the degradation of polycyclic aromatic hydrocarbons in dilute water streams," *Journal of Hazardous Materials*, vol. 99, no. 2, pp. 203–219, 2003.
- [15] S. Dass, M. Muneer, and K. R. Gopidas, "Photocatalytic degradation of wastewater pollutants. Titanium-dioxide-mediated oxidation of polynuclear aromatic hydrocarbons," *Journal of Photochemistry and Photobiology A: Chemistry*, vol. 77, no. 1, pp. 83–88, 1994.
- [16] A. Lair, C. Ferronato, J.-M. Chovelon, and J.-M. Herrmann, "Naphthalene degradation in water by heterogeneous photocatalysis: an investigation of the influence of inorganic anions," *Journal of Photochemistry and Photobiology A: Chemistry*, vol. 193, no. 2–3, pp. 193–203, 2008.
- [17] O. T. Woo, W. K. Chung, K. H. Wong, A. T. Chow, and P. K. Wong, "Photocatalytic oxidation of polycyclic aromatic hydrocarbons: intermediates identification and toxicity testing," *Journal of Hazardous Materials*, vol. 168, no. 2–3, pp. 1192–1199, 2009.
- [18] N. Vela, M. Martínez-Menchón, G. Navarro, G. Pérez-Lucas, and S. Navarro, "Removal of polycyclic aromatic hydrocarbons (PAHs) from groundwater by heterogeneous photocatalysis under natural sunlight," *Journal of Photochemistry and Photobiology A: Chemistry*, vol. 232, pp. 32–40, 2012.
- [19] H. Tong, S. Ouyang, Y. Bi, N. Umezawa, M. Oshikiri, and J. Ye, "Nano-photocatalytic materials: possibilities and challenges," *Advanced Materials*, vol. 24, no. 2, pp. 229–251, 2012.
- [20] D. Bahnemann, "Photocatalytic water treatment: solar energy applications," *Solar Energy*, vol. 77, no. 5, pp. 445–459, 2004.
- [21] A. Matsuda, S. Sreekantan, and W. Krengvirat, "Well-aligned TiO₂ nanotube arrays for energy-related applications under solar irradiation," *Journal of Asian Ceramic Societies*, vol. 1, no. 3, pp. 203–219, 2013.
- [22] Y.-K. Lai, J.-Y. Huang, H.-F. Zhang et al., "Nitrogen-doped TiO₂ nanotube array films with enhanced photocatalytic activity under various light sources," *Journal of Hazardous Materials*, vol. 184, no. 1–3, pp. 855–863, 2010.
- [23] Y. Lai, L. Sun, Y. Chen, H. Zhuang, C. Lin, and J. W. Chin, "Effects of the structure of TiO₂ nanotube array on Ti substrate on its photocatalytic activity," *Journal of the Electrochemical Society*, vol. 153, no. 7, pp. D123–D127, 2006.
- [24] D. Yu, B. Bo, and Y. He, "Fabrication of TiO₂ yeast-carbon hybrid composites with the raspberry-like structure and their synergistic adsorption-photocatalysis performance," *Journal of Nanomaterials*, vol. 2013, Article ID 851417, 8 pages, 2013.
- [25] C. Hu, Y. Wang, and H. Tang, "Preparation and characterization of surface bond-conjugated TiO₂/SiO₂ and photocatalysis for azo dyes," *Applied Catalysis B: Environmental*, vol. 30, pp. 277–285, 2001.
- [26] K. Balachandaran, R. Venkatesh, and R. Sivaraj, "Synthesis of nano TiO₂-SiO₂ composite using sol-gel method: effect on size, surface morphology and thermal stability," *International Journal of Engineering Science and Technology*, vol. 2, no. 8, pp. 3695–3700, 2010.
- [27] Y. Guo, S. Yang, X. Zhou, C. Lin, Y. Wang, and W. Zhang, "Enhanced photocatalytic activity for degradation of methyl orange over silica-titania," *Journal of Nanomaterials*, vol. 2011, Article ID 296953, 9 pages, 2011.
- [28] Y. Ishibai, J. Sato, S. Akita, T. Nishikawa, and S. Miyagishi, "Photocatalytic oxidation of NO_x by Pt-modified TiO₂ under visible light irradiation," *Journal of Photochemistry and Photobiology A: Chemistry*, vol. 188, no. 1, pp. 106–111, 2007.
- [29] S. P. Devipriya, S. Yesodharan, and E. P. Yesodharan, "Solar photocatalytic removal of chemical and bacterial pollutants from water using Pt/TiO₂-coated ceramic tiles," *International Journal of Photoenergy*, vol. 2012, Article ID 970474, 8 pages, 2012.
- [30] L. M. Ahmed, I. Ivanova, F. H. Hussein, and D. W. Bahnemann, "Role of platinum deposited on TiO₂ in photocatalytic methanol oxidation and dehydrogenation reactions," *International Journal of Photoenergy*, vol. 2014, Article ID 503516, 9 pages, 2014.
- [31] M. Ni, M. K. H. Leung, D. Y. C. Leung, and K. Sumathy, "A review and recent developments in photocatalytic water-splitting using TiO₂ for hydrogen production," *Renewable and Sustainable Energy Reviews*, vol. 11, no. 3, pp. 401–425, 2007.
- [32] NCB, "The National Center for Biotechnology-PubChem Compound," <http://pubchem.ncbi.nlm.nih.gov/summary/summary.cgi?cid=995#itabs=3d>.
- [33] E. Martínez, M. Gros, S. Lacorte, and D. Barceló, "Simplified procedures for the analysis of polycyclic aromatic hydrocarbons in water, sediments and mussels," *Journal of Chromatography A*, vol. 1047, no. 2, pp. 181–188, 2004.

- [34] Z. Luo, K. Katayama-Hirayama, T. Akitsu, and H. Kaneko, "Photocatalytic degradation of pyrene in porous Pt/TiO₂-SiO₂ photocatalyst suspension under UV irradiation," *Nano*, vol. 3, no. 5, pp. 317–322, 2008.
- [35] Z. Luo, K. Katayama-Hirayama, K. Hirayama, T. Akitsu, and H. Kaneko, "Preparation of porous Pt/TiO₂-SiO₂ photocatalyst and its performance in photocatalytic degradation of pyrene," *International Journal of Plasma Environmental Science & Technology*, vol. 2, no. 2, pp. 77–81, 2008.
- [36] J. Chen, W. J. G. M. Peijnenburg, X. Quan et al., "Is it possible to develop a QSPR model for direct photolysis half-lives of PAHs under irradiation of sunlight?" *Environmental Pollution*, vol. 114, no. 1, pp. 137–143, 2001.
- [37] C. Raillard, V. Héquet, B. Gao et al., "Correlations between molecular descriptors from various volatile organic compounds and photocatalytic oxidation kinetic constants," *International Journal of Chemical Reactor Engineering*, vol. 11, no. 2, pp. 799–813, 2013.
- [38] G.-H. Lu, C. Wang, and X.-L. Guo, "Prediction of toxicity of phenols and anilines to algae by quantitative structure-activity relationship," *Biomedical and Environmental Sciences*, vol. 21, no. 3, pp. 193–196, 2008.
- [39] J.-Y. Hu and T. Aizawa, "Quantitative structure-activity relationships for estrogen receptor binding affinity of phenolic chemicals," *Water Research*, vol. 37, no. 6, pp. 1213–1222, 2003.
- [40] F. A. de Lima Ribeiro and M. M. C. Ferreira, "QSAR model of the phototoxicity of polycyclic aromatic hydrocarbons," *Journal of Molecular Structure: THEOCHEM*, vol. 719, no. 1–3, pp. 191–200, 2005.
- [41] J. Chen, X. Quan, W. J. G. M. Peijnenburg, and F. Yang, "Quantitative structure-property relationships (QSPRs) on direct photolysis quantum yields of PCDDs," *Chemosphere*, vol. 43, no. 2, pp. 235–241, 2001.
- [42] J. Chen, X. Quan, Y. Yan, F. Yang, and W. J. G. M. Peijnenburg, "Quantitative structure-property relationship studies on direct photolysis of selected polycyclic aromatic hydrocarbons in atmospheric aerosol," *Chemosphere*, vol. 42, no. 3, pp. 263–270, 2001.
- [43] J. Chen, W. J. G. M. Peijnenburg, X. Quan, and F. Yang, "Quantitative structure-property relationships for direct photolysis quantum yields of selected polycyclic aromatic hydrocarbons," *Science of The Total Environment*, vol. 246, no. 1, pp. 11–20, 2000.
- [44] J. Chen, D. Wang, S. Wang, X. Qiao, and L. Huang, "Quantitative structure-property relationships for direct photolysis of polybrominated diphenyl ethers," *Ecotoxicology and Environmental Safety*, vol. 66, no. 3, pp. 348–352, 2007.
- [45] G. D. Veith, O. G. Mekenyan, G. T. Ankley, and D. J. Call, "A QSAR analysis of substituent effects on the photoinduced acute toxicity of PAHs," *Chemosphere*, vol. 30, no. 11, pp. 2129–2142, 1995.
- [46] O. G. Mekenyan, G. T. Ankley, G. D. Veith, and D. J. Call, "QSARs for photo-induced toxicity: I—acute lethality of polycyclic aromatic hydrocarbons to *Daphnia magna*," *Chemosphere*, vol. 28, no. 3, pp. 567–582, 1994.
- [47] B.-C. Wang, J.-C. Chang, H.-C. Tso, H.-F. Hsu, and C.-Y. Cheng, "Theoretical investigation the electroluminescence characteristics of pyrene and its derivatives," *Journal of Molecular Structure: THEOCHEM*, vol. 629, no. 1–3, pp. 11–20, 2003.
- [48] H. Wang, C. Wang, W. Wu, Z. Mo, and Z. Wang, "Persistent organic pollutants in water and surface sediments of Taihu Lake, China and risk assessment," *Chemosphere*, vol. 50, no. 4, pp. 557–562, 2003.
- [49] Y. Li, J. Niu, L. Yin et al., "Photocatalytic degradation kinetics and mechanism of pentachlorophenol based on Superoxide radicals," *Journal of Environmental Sciences*, vol. 23, no. 11, pp. 1911–1918, 2011.
- [50] J. Sabaté, J. M. Bayona, and A. M. Solanas, "Photolysis of PAHs in aqueous phase by UV irradiation," *Chemosphere*, vol. 44, no. 2, pp. 119–124, 2001.
- [51] N. Das and P. Chandran, "Microbial degradation of petroleum hydrocarbon contaminants: an overview," *Biotechnology Research International*, vol. 2011, Article ID 941810, 13 pages, 2011.
- [52] J.-S. Seo, Y.-S. Keum, and Q. X. Li, "Bacterial degradation of aromatic compounds," *International Journal of Environmental Research and Public Health*, vol. 6, no. 1, pp. 278–309, 2009.
- [53] Y. Mei, F. Wu, L. Wang, Y. Bai, W. Li, and H. Liao, "Binding characteristics of perylene, phenanthrene and anthracene to different DOM fractions from lake water," *Journal of Environmental Sciences*, vol. 21, no. 4, pp. 414–423, 2009.

